[CANCER RESEARCH 60, 5649–5658, October 15, 2000]

Melanoma-targeting Properties of ^{99m}Technetium-labeled Cyclic α-Melanocyte-stimulating Hormone Peptide Analogues[1]

JianQing Chen, Zhen Cheng, Timothy J. Hoffman, Silvia S. Jurisson, and Thomas P. Quinn[2]

Departments of Biochemistry [JQ. C., T. P. Q.] and Chemistry [Z. C., S. S. J.], University of Missouri-Columbia, Columbia, Missouri 65211, and Harry S. Truman Memorial Veterans Hospital, Columbia, Missouri 65201 [T. J. H.]

ABSTRACT

Preliminary reports have demonstrated that ^{99m}technetium (Tc)-labeled cyclic [Cys^{3,4,10}, D-Phe^7]α-MSH$_{3-13}$ (CCMSH) exhibits high tumor uptake and retention values in a murine melanoma mouse model. In this report, the tumor targeting mechanism of ^{99m}Tc-CCMSH was studied and compared with four other radiolabeled α-melanocyte stimulating hormone (α-MSH) peptide analogues: ^{125}I-(Tyr^2)-[Nle^4, D-Phe^7]α-MSH [^{125}I-(Tyr^2)-NDP]; ^{99m}Tc-CGCG-NDP; ^{99m}Tc-Gly^{11}-CCMSH; and ^{99m}Tc-Nle^{11}-CCMSH. *In vitro* receptor binding, internalization, and cellular retention of radiolabeled α-MSH analogues in B16/F1 murine cell line demonstrated that >70% of the receptor-bound radiolabeled analogues were internalized together with the receptor. Ninety % of the internalized ^{125}I-(Tyr^2)-NDP, whereas only 36% of internalized ^{99m}Tc-CCMSH, was released from the cells into the medium during a 4-h incubation at 37°C. Two mouse models, C57 mice and severe combined immunodeficient (Scid) mice, inoculated s.c. with B16/F1 murine and TXM-13 human melanoma cells were used for the *in vivo* studies. Tumor uptake values of 11.32 and 2.39 [% injected dose (ID)/g] for ^{99m}Tc-CCMSH at 4 h after injection, resulted in an uptake ratio of tumor:blood of 39.0 and 11.5 in murine melanoma-C57 and human melanoma-Scid mouse models, respectively. Two strategies for decreasing the nonspecific kidney uptake of ^{99m}Tc-CCMSH, substitution of Lys^{11} in CCMSH with Gly^{11} or Nle^{11}, and lysine coinjection, were evaluated. The biodistribution data for the modified peptides showed that Lys^{11} replacement dramatically decreased the kidney uptake, whereas the tumor uptakes of ^{99m}Tc-Nle^{11}- and ^{99m}Tc-Gly^{11}-CCMSH were significantly lower than that of ^{99m}Tc-CCMSH. Lysine coinjection significantly decreased the kidney uptake (*e.g.*, from 14.6% ID/g to 4.5% ID/g at 4 h after injection in murine melanoma-C57 mice) without significantly changing the value of tumor uptake of ^{99m}Tc-CCMSH. In conclusion, the compact cyclic structure of ^{99m}Tc-CCMSH, its resistance to degradation, and its enhanced intracellular retention are the major contributing factors to the superior *in vivo* tumor targeting properties of ^{99m}Tc-CCMSH. Lys^{11} residue in ^{99m}Tc-CCMSH is critical to the tumor targeting *in vivo*, and lysine coinjection rather than lysine replacement can significantly decrease the nonspecific renal radioactivity accumulation without impeding the high melanoma-targeting properties of ^{99m}Tc-CCMSH. The metal-cyclized CCMSH molecule displays excellent potential for the development of melanoma-specific diagnostic and therapeutic agents.

INTRODUCTION

Malignant melanoma has become a severe public health problem because of an increase in incidence and the difficulties in discovering and treating melanoma metastases (1, 2). In recent years, with the identification of melanoma-associated antigens and the development of anti-melanoma antibodies, radioimmunodetection for melanoma and its metastases via radiolabeled antibodies and antibody fragments has been investigated extensively (3–5). Radioimmunodetection has been successfully used for imaging known metastatic melanoma lesions with sizes >1.0 cm (6, 7). However, difficulties in the detection of smaller lesions remain because of the intrinsic limitations of radiolabeled antibodies and antibody fragments, such as slow circulation clearance (8, 9), reduced rates of tumor penetration (10, 11), and their antigenicity (12).

An alternative approach for tumor targeting is the use of lower molecular weight, high-affinity receptor binding ligands, such as peptides, for tumor-selective delivery of radionuclides (13, 14). For instance, the receptor for α-MSH[3] is found on murine (15) and human melanoma cells (16). It has been reported that >80% of human melanoma tumor samples obtained from patients with metastatic melanoma bear α-MSH receptors (17), enabling the use of radiolabeled α-MSH peptide analogues as specific melanoma diagnostic and therapeutic agents. Wild-type α-MSH (Ac-Ser^1-Tyr^2-Ser^3-Met^4-Glu^5-His^6-Phe^7-Arg^8-Trp^9-Gly^{10}-Lys^{11}-Pro^{12}-Val^{13}-NH$_2$) is a tridecapeptide that is primarily responsible for the regulation of skin pigmentation (18). Several superpotent α-MSH analogues have been synthesized that possess increased receptor affinity and stability (19, 20). For example, substitution of Met^4 with Nle^4 and Phe^7 with D-Phe^7 yields the NDP analogue, which is one of the most cited α-MSH analogues because of its subnanomolar receptor affinity and resistance to enzymatic degradation (16, 19). It has also been reported that α-MSH peptides cyclized via disulfide bond [Cys (4, 10), D-Phe^7]α-MSH (20) or lactam bond formation [Asp^5, D-Phe^7, Lys^{11}]α-MSH (21, 22) display increased receptor binding affinity and resistance to proteolysis. High receptor affinity and stability have made these α-MSH analogues attractive as site-specific delivery vehicles for radionuclides, toxins, and chemotherapeutic molecules (23, 24).

Recently, several radiolabeled α-MSH peptide analogues have been investigated for melanoma-specific targeting. Direct halogenation of NDP with ^{125}I at Tyr^2 resulted in a radioiodinated α-MSH analogue with excellent cell-binding characteristics *in vitro* (25), but it was subject to dehalogenation *in vivo*. Dehalogenation has been largely overcome by labeling NDP with succinimidyl 3- or 4-(^{125}I or ^{18}F) benzoate, yielding molecules that display significant improvements in stability and clearance from normal tissues (26, 27). ^{111}In-labeled α-MSH derivatives containing two NDP sequences linked together via a single DTPA molecule have been examined for their abilities to image the melanoma lesions in patients (14). Although the ^{111}In-labeled DTPA-bis-NDP conjugates were able to image melanoma tumors *in vivo*, routine clinical use appears limited because of high nonspecific radioactivity accumulation in the liver and kidneys (28). To decrease the background in the liver and kidneys, ^{111}In-labeled DTPA-mono-NDP has also been investigated (29). However, the tumor uptake of ^{111}In-labeled DTPA-mono-NDP was significantly lower than that of ^{111}In-labeled DTPA-bis-NDP. Our previous results with ^{99m}Tc/^{188}Re-NDP, labeled with either the CGCG chelating tet-

Received 3/7/00; accepted 8/17/00.

The costs of publication of this article were defrayed in part by the payment of page charges. This article must therefore be hereby marked *advertisement* in accordance with 18 U.S.C. Section 1734 solely to indicate this fact.

[1] Supported by Grant ER61661 from the Department of Energy (to T. P. Q.) and a grant from the University of Missouri Molecular Biology Postdoctoral Fellowship (to JQ. C.).

[2] To whom requests for reprints should be addressed, at Department of Biochemistry, 117 Schweitzer Hall, University of Missouri-Columbia, Columbia, MO 65211. Phone: (573) 882-6099; Fax: (573) 882-5635; E-mail: quinnt@missouri.edu.

[3] The abbreviations used are: α-MSH, α-melanocyte stimulating hormone; DTPA, diethylenetriaminepentaacetic acid; CGCG, Ac-Cys-Gly-Cys-Gly; Scid, severe combined immunodeficient; HPLC, high-performance liquid chromatography; RP, reverse phase; TFA, trifluoroacetic acid; GI, gastrointestinal tract; ID, injected dose; FAB, fast atom bombardment; NDP, [Nle^4, D-Phe^7]α-MSH; CCMSH, [Cys^{3,4,10}, D-Phe^7]α-MSH$_{3-13}$; Gly^{11}-CCMSH, [Cys^{3,4,10}, D-Phe^7, Gly^{11}]α-MSH$_{3-13}$; Nle^{11}-CCMSH, [Cys^{3,4,10}, D-Phe^7, Nle^{11}]α-MSH$_{3-13}$.

rapeptide (30) or MAG_2 chelate (tetrafluorophenyl mercapto-acetyl-glycylglycyl-γ-aminobutyrate), illustrated that tumor-targeted radioactivity was rapidly washed out of the tumor tissue (31).

Significantly higher tumor uptake values were obtained for ^{99m}Tc/^{188}Re-labeled CCMSH, an 11-amino acid α-MSH peptide analogue cyclized via metal coordination with three $Cys^{3,4,10}$ sulfhydryls and one Cys^4 amide nitrogen positioned in the sequence of the peptide (23, 32). The ^{99m}Tc/^{188}Re-CCMSH exhibited excellent tumor radioactivity retention and fast whole body clearance via the kidneys into the urine. However, significant kidney radioactivity accumulation was observed, which could limit the therapeutic index if a β- or α-emitting radionuclide is coordinated to the peptide for therapeutic purposes.

In this study, the mechanism of ^{99m}Tc-CCMSH tumor uptake was studied by characterizing the receptor binding, internalization, and cellular retention of the radiolabeled complex in B16/F1 murine melanoma cells *in vitro* and compared with ^{125}I-(Tyr^2)-NDP and ^{99m}Tc-CGCG-NDP. Self-regulation of the α-MSH receptor by NDP and receptor recovery was also investigated. The *in vivo* tumor targeting capacity of ^{99m}Tc-CCMSH was evaluated in both C57 BL/6 and Fox Chase ICR Scid mouse melanoma models, inoculated s.c. with B16/F1 murine and TXM-13 human melanoma cells and compared with that of ^{125}I-(Tyr^2)-NDP and ^{99m}Tc-CGCG-NDP. The specificity of ^{99m}Tc-CCMSH tumor uptakes was determined *in vivo* by a coinjection of 2 μg of nonradiolabeled NDP. In addition, two strategies of blocking nonspecific kidney uptake of ^{99m}Tc-CCMSH were examined. One of the strategies involved the replacement of Lys^{11} in CCMSH with Nle^{11} or Gly^{11}. The *in vitro* receptor binding affinity (IC_{50}) and *in vivo* biodistribution of the modified peptides, ^{99m}Tc-Nle^{11}-CCMSH and ^{99m}Tc-Gly^{11}-CCMSH, were tested and compared with those of ^{99m}Tc-CCMSH. The other strategy investigated for reducing nonspecific renal uptake was lysine coinjection. Blocking the nonspecific kidney uptake with two different quantities and times of lysine injection was examined in healthy C57 mice and then in B16/F1 melanoma-bearing mice. Tumor imaging was performed at 1 and 8 h after the administration of ^{99m}Tc-CCMSH in murine melanoma-bearing C57 mice.

MATERIALS AND METHODS

Peptides Synthesis. Peptides CCMSH, Gly^{11}-CCMSH, Nle^{11}-CCMSH, NDP, and CGCG-NDP were synthesized using fluorenylmethoxycarbonyl/2(1*H*-benzotriazol-1-ly)-1,1,3,3,tetramethyluronium hexafluorophosphate solid-phase peptide synthesis chemistry on amide resin with a Synergy 432A desktop peptide synthesizer from Applied Biosystems (Foster City, CA). Protected amino acids were purchased from Advanced ChemTech, Inc. (Louisville, KY). Peptides were acetylated by activating glacial acetic acid with 2(1*H*-benzotriazol-1-ly)-1,1,3,3,tetramethyluronium hexafluorophosphate after deprotecting the NH_2-terminal residue. For peptide cleavage and deprotection, the peptide-resin was stirred in a mixture of TFA:thioanisole:ethanedithiol:H_2O (in a ratio of 36:2:1:1 by volume) at room temperature for 2 h. The peptide in the solution was precipitated and washed four times with ice-cold diethyl ether. After drying and then dissolving in 1 mM DTT, the peptide was purified by HPLC (Isco, Inc., Lincoln, NE) on a C-18 RP column (218TP54; Vydac, Hesperia, CA). The purified peptides were lyophilized and stored at −20°C. Peptide identities were confirmed by FAB mass spectrometry (Mass Spectrometric Analytic Laboratory, University of Kansas, Lawrence, KS).

Preparation of Radiolabeled Complexes. ^{125}I-(Tyr^2)-NDP (2000 Ci/mmol) was obtained from Advanced ChemTech (Louisville, KY). ^{99m}Tc-labeled CCMSH, Gly^{11}-CCMSH, Nle^{11}-CCMSH, and CGCG-NDP were prepared by using stannous chloride as a reducing agent and glucoheptonate as a transfer ligand. Briefly, 30 μl of 2 mg/ml $SnCl_2$ in 0.2 M glucoheptonate were added into 200 μl of fresh $^{99m}TcO_4^-$ eluate from a ^{99} Mo/^{99m}Tc generator (1–4 mCi). After the formation of ^{99m}Tc-glucoheptonate and the adjustment of the pH to 9 with 0.1 M NaOH, 10 μg of the peptide were added, and the reaction mixture was incubated at 75°C for 30 min. The radiolabeled complex was purified by HPLC using a C-18 RP column. A 20-min gradient of 17–22% acetonitrile/0.1% TFA *versus* H_2O/0.1% TFA was used for the purification of ^{99m}Tc-CCMSH, and a 20-min gradient of 20–25% or 24–29% acetonitrile/0.1% TFA *versus* H_2O/0.1% TFA was used for the purification of ^{99m}Tc-Gly^{11}-CCMSH, ^{99m}Tc-Nle^{11}-CCMSH, or ^{99m}Tc-CGCG-MSH, respectively. Purified preparations were flushed with nitrogen gas to remove the acetonitrile, and the pH was adjusted to 7 by addition of 0.2 M sodium phosphate (pH 8.0)/150 mM NaCl. The stability of the radiolabeled complexes was evaluated in 0.01 M, pH 7.4 PBS.

Cell Culture. B16/F1 murine melanoma cells were obtained from American Type Tissue Culture Collection, and human TXM-13 melanoma cells were supplied by Dr. Isaiah J. Fidler from the Cell Biology Department, University of Texas M. D. Anderson Cancer Center. The human melanoma line TXM-13JQ was derived from the parent cell line TXM-13 after successive passages *in vitro*. Melanoma cells were cultured in RPMI 1640 containing $NaHCO_3$ (2 g/l), which was supplemented with 10% heat-inactivated FCS, 2 mM L-glutamine, and 48 mg of gentamicin. The cells were expanded in 75-cm^2 tissue culture flasks and kept in a humidified atmosphere of 5% CO_2 at 37°C. The media were changed every other day. A confluent monolayer was detached with 0.02% EDTA in Ca^{2+} and Mg^{2+} free, pH 7.4, 0.01 M PBS and dissociated into a single-cell suspension for further cell culture.

***In Vitro* Cell Assays.** Receptor binding affinity, internalization and cellular retention assays were performed on B16/F1 murine cells. Cell binding experiments were performed as follows. Cells were seeded at a density of 0.2 million/well in 24-well tissue culture plates and allowed to attach overnight. After washing once with the binding medium [MEM with 25 mM HEPES, 0.2% BSA, and 0.3 mM 1,10-phenanthroline (Sigma, St. Louis, MO)], the cells were incubated at 25°C for 3 h with ~50,000 cpm of ^{125}I-(Tyr^2)-NDP or 200,000 cpm of the ^{99m}Tc-labeled analogues in 0.5 ml of binding medium. The nonspecific binding was determined by coincubation with nonradiolabeled NDP at a final concentration of 10 μM. The cells were rinsed twice with pH 7.4, 0.01 M PBS/0.2% BSA and lysed in 0.5 ml of 1 M NaOH for 5 min, and their radioactivity was measured.

Internalization and cellular retention of ^{99m}Tc-CCMSH was evaluated and compared with ^{99m}Tc-CGCG-NDP and ^{125}I-(Tyr^2)-NDP in B16/F1 murine melanoma cells. The cells were prepared as described above in 24-well tissue culture plates and incubated at 25°C for a period of 5 min to 4 h in 0.5 ml of binding media with ~50,000 cpm of ^{125}I-labeled or 200,000 cpm of the ^{99m}Tc-labeled complexes. Internalization of the radiolabeled complex was assessed by washing the cells with acid buffer [40 mM sodium acetate (pH 4.5) containing 0.9% NaCl and 0.2% BSA] to remove the membrane bound radiocomplex, and the remaining internalized radioactivity in the cells was measured. The cellular retention properties of the internalized ^{125}I- or ^{99m}Tc-labeled α-MSH analogues were determined by incubating B16/F1 cells with the radiolabeled analogues for 3 h, removing the membrane-bound radioactivity with acid buffer wash, and monitoring radioactivity release into the media at 25°C or 37°C. At different time points over a 4-h incubation period, the radioactivity in the medium and in the cells were separately collected and counted. The radioactive moiety in the medium was analyzed using a C-18 Sep-Pak Cartridge (Water Corporation, MA). After equilibrating the cartridge with 10% acetonitrile/H_2O, 200 μl of the sample were loaded onto the column, which was then rinsed with 3 ml of 10% acetonitrile/H_2O, followed by 3 ml of 60% acetonitrile/H_2O. Free $^{99m}TcO_4^-$, ^{99m}Tc-labeled analogues, and ^{125}I-(Tyr^2)-NDP were used as controls.

Self-regulation of α-MSH receptors by NDP was examined in B16/F1 cells. Cells were treated for 24 h in RPMI 1640 supplemented with 10% dialyzed FCS (10,000 molecular weight cutoff dialyzed FCF; Sigma Chemical Co., St. Louis, MO) or in 10% normal FCS-supplemented RPMI 1640 containing NDP at a concentration of 20 or 50 nM. After removal of the membrane-bound NDP by washing the cells with acid buffer, the cells were further cultured in medium. At different time points within a period of 96 h, the binding capacity of the treated cells for ^{125}I-(Tyr^2)-NDP was determined.

The IC_{50}, the concentration of competitor required to inhibit 50% of radioligand binding, of CCMSH, ReCCMSH, Gly^{11}-CCMSH, and Nle^{11}-CCMSH was determined in competitive binding assays with ^{125}I-(Tyr^2)-NDP over a 10^{-14}–10^{-6} (M) concentration range. The Bmax of B16/F1 and TXM-13 cells was determined by incubating a fixed number of cells with serial concentrations of ^{125}I-(Tyr^2)-NDP under the receptor binding conditions described above. Meanwhile, the binding fraction (1/*r*) of ^{125}I-(Tyr^2)-NDP to

B16/F1 cells was assayed according to a method that was developed to determine the immunoreactive fraction of radiolabeled antibodies (33). Briefly, serially diluted B16/F1 cells suspensions (0.125–16 million) in 0.5 ml of binding medium were incubated with a certain concentration of ^{125}I-(Tyr^2)-NDP at 25°C for 3 h. Total applied radioactivity over specific binding (total/specific binding) was used as a function of the reverse cell concentration (ml/million), and *r* was obtained by linear extrapolation to the ordinate.

***In Vivo* Biodistribution, Imaging, and Tumor Tissue Histopathological Studies.** C57 BL/6 and Fox Chase ICR Scid female mice (Harlan Sprague Dawley, Indianapolis, IN) were inoculated s.c. in the right flank with 1×10^6 cultured B16/F1 murine and TXM-13JQ human melanoma cells, respectively. Ten days after the inoculation, tumors reached a weight of ~500 mg. It took 4 weeks for the TXM-13 human melanoma tumors to reach a weight of ~500 mg, induced by s.c. inoculation with 3×10^6 cells in Scid mice. Two to four μCi of ^{99m}Tc- or ^{125}I-labeled peptide (72,000 Ci/mmol or 2,000 Ci/mmol, with a corresponding peptide amount of 0.065 or 2.6 ng, respectively) was injected into each mouse through the tail vein for biodistribution and *in vivo* tumor targeting studies. About 20 μCi of ^{99m}Tc-peptide was administrated into each mouse for the 24-h postinjection group. After injection, the mice were housed separately, and their urine and feces were collected. Groups of five mice were sacrificed at different time points after injection. Tumor and normal tissues of interest were dissected, and the blood on the samples was sponged off with gauze. The contents in the GI were not removed. Tissue samples and the carcass were weighed, and their radioactivity was measured in a gamma counter, together with the collected urine and feces. The total blood value was counted as 6.5% of the whole body weight. The radioactivity uptake in the tumor and normal tissues of interest was expressed as a percentage of the injected radioactivity dose per gram of tissue (% ID/g) or percentage of the injected dose (% ID). The specificity of the *in vivo* tumor uptake of ^{99m}Tc-CCMSH was determined by a coinjection with 2 μg of nonradiolabeled NDP, a 30,000 fold molar excess to ^{99m}Tc-CCMSH.

The effect of lysine coinjection on the reduction of nonspecific kidney uptake of ^{99m}Tc-CCMSH was determined in healthy C57 BL/6 mice. Group 1 was i.p. injected with 20 mg of lysine (L-lysine monohydrochloride; Fisher Biotech, Houston, TX), and 5 min later injected with a mixture of ^{99m}Tc-CCMSH and 25 mg of lysine through the tail vein. Group 2 was i.v. injected with a mixture of ^{99m}Tc-CCMSH and 25 mg of lysine only. A single injection of ^{99m}Tc-CCMSH with 30 mg of lysine was used for further studies in the tumor model to check whether the lysine coinjection would interfere with the tumor targeting property of ^{99m}Tc-CCMSH.

In the imaging studies, mice were injected with 100 μCi of ^{99m}Tc-CCMSH through the tail vein. Mouse images were acquired at 1 and 8 h after injection by a Siemens LEM + Mobile γ camera equipped with a low energy parallel hole collimator. The images were collected on a 512 matrix with ×1.5 magnification and 8-bit depth.

For histopathological examination, the tumor tissues were dissected and then immediately fixed in buffered 10% formalin. The fixed tumor tissue was sliced in a thickness of 5 μm and stained in H&E staining. Histopathological studies were performed by the Research Animal Diagnostic and Investigative Laboratory (University of Missouri, Columbia, MO).

All of the animal studies were carried out in compliance with Federal and local institutional rules for the conduct of animal experimentation. Statistical analysis was performed using the Student's *t* test for unpaired data.

Table 1 *Sequences of α-MSH analogues involved in this investigation and their molecular weights (MW) calculated and measured by FAB mass spectrometry*

Analogue	Sequence	Calculated (MW)	Measured (MWH$^+$)
α-MSH	Ac-SYSMEHFRWGKPV-NH$_2$	1665	ND
NDP	Ac-SYS(Nle)EHdFRWGKPV-NH$_2$	1647	1648.7
CGCG-NDP	Ac-CGCGSYS(Nle)EHdFRWGKPV-NH$_2$	1975	1976.8
CCMSH	Ac-CCEHdFRWCKPV-NH$_2$	1447	1448
Gly^{11}-CCMSH	Ac-CCEHdFRWCGPV-NH$_2$	1376	1377.6
Nle^{11}-CCMSH[a]	Ac-CCEHdFRWC(Nle)PV-NH$_2$	1432	1433
^{125}I-Tyr^2-NDP	Ac-S(^{125}I)YS(Nle)EHdFRWGKPV-NH$_2$	1772	ND

[a] Nle, norleucine.

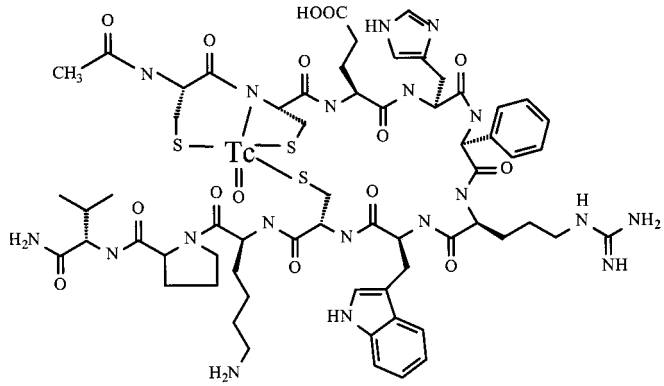

Fig. 1. A structural model of ^{99m}Tc-CCMSH; Acetyl-Cys-Cys-Glu-His-dPhe-Arg-Trp-Cys-Lys-Pro-Val-NH$_2$.

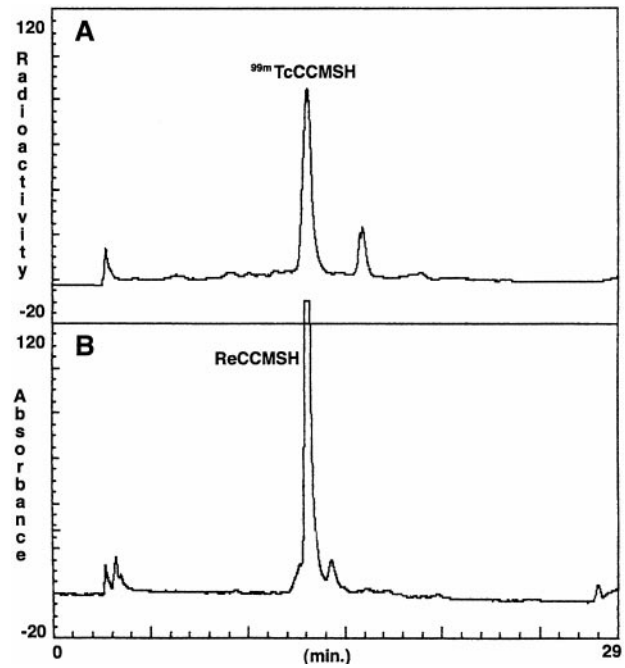

Fig. 2. HPLC analysis of a ^{99m}Tc-CCMSH radiolabeling reaction, which was coinjected with nuclear magnetic resonance-confirmed Re-CCMSH standard.

RESULTS

All of the α-MSH analogues, except ^{125}I-(Tyr^2)-NDP, were synthesized by solid-phase Fmoc synthesis, purified by RP-HPLC and characterized by FAB mass spectrometry. Table 1 lists the sequences used in this study and the calculated and measured molecular weights of the α-MSH analogues. The ^{99m}Tc-labeled peptides were completely separated from their nonradiolabeled counterparts by RP-HPLC because of an increase in hydrophobicity. The structure of metal-cyclized ^{99m}Tc-CCMSH is shown in Fig. 1. In addition to mass spectrometry, the identity of the ^{99m}Tc-CCMSH was confirmed by analytical HPLC analysis. A Re-CCMSH nuclear magnetic resonance standard sample was coinjected with a ^{99m}Tc-CCMSH radiolabeling reaction mixture. The major product of the ^{99m}Tc-CCMSH reaction comigrated with the Re-CCMSH standard (Fig. 2). A similar analytic HPLC analysis, using a Re-CGCG-NDP synthetic standard (30), was used to confirm the identity of the ^{99m}Tc-CGCG-NDP (data not shown). The radiochemical stability of all of the ^{99m}Tc-labeled analogues was evaluated in pH 7.4, PBS. Over a 24-h period of incubation at 25°C in PBS, only radiolabeled peptide and no detectable free radioactivity was observed by RP-HPLC.

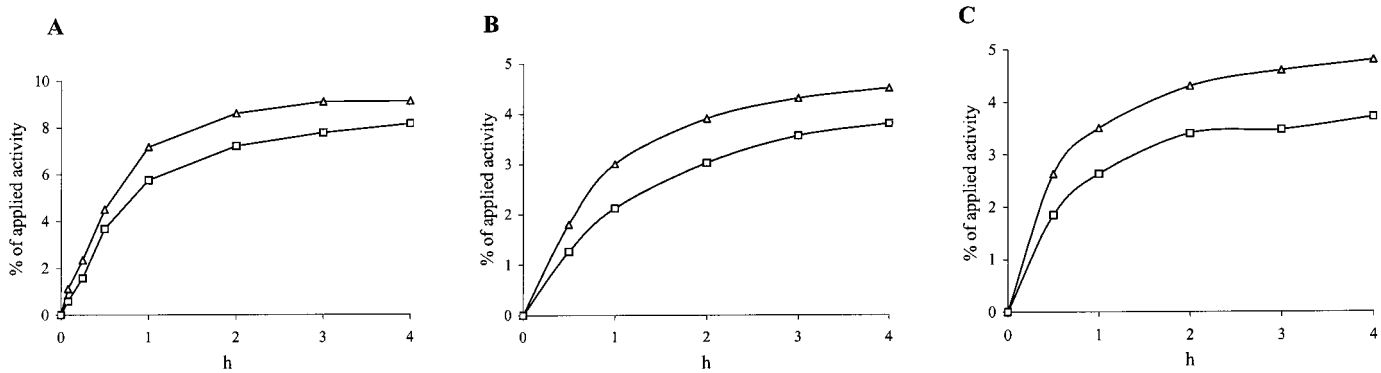

Fig. 3. Cell binding and internalization over time for ^{125}I-(Tyr^2)-NDP (*A*) ^{99m}Tc-CCMSH (*B*) and ^{99m}Tc-CGCG-NDP (*C*) on B16/F1 cells at 25°C. Bound radioactivity (△) and internalized activity (□) are expressed as a percentage of applied activity.

Cell Binding and Internalization. Fig. 3 shows the cell binding and internalization of ^{125}I-(Tyr^2)-NDP (Fig. 3*A*), ^{99m}Tc-CCMSH (Fig. 3*B*), and ^{99m}Tc-CGCG-NDP (Fig. 3*C*) on B16/F1 cells at 25°C over a 4-h incubation period. Four to 8% cell binding was obtained for all three radiolabeled analogues with 3 h incubation. The internalization was assessed after removal of free and membrane-bound radioactivity by washing the cells with pH 4.5, 40 mM sodium acetate acid buffer and collecting the remaining cellular radioactivity. Approximately 70% of the receptor-bound radiolabeled complexes was internalized as early as 5 min after incubation for the ^{125}I-(Tyr^2)-NDP in B16/F1 cells. Although receptor binding increased over the incubation period, the percentages of the radioactivity internalized *versus* total binding did not significantly change. Similar results were observed among the three ^{99m}Tc- and ^{125}I-labeled analogues.

Cellular Retention. Cellular retention of the radiolabeled analogues was analyzed and compared in B16/F1 cells. After reaching the maximal binding, the membrane-bound radioactivity was removed with an acid buffer wash, and the cells were returned to cell culture medium and incubated at 25°C or 37°C. Fig. 4 illustrates the cellular radioactive retention of ^{99m}Tc-CCMSH, ^{99m}Tc-CGCG-NDP, and ^{125}I-(Tyr^2)-NDP in B16/F1 cells over time at different temperatures. Approximately 36% of the internalized radioactivity of ^{99m}Tc-CCMSH and ^{99m}Tc-CGCG-NDP and 90% of the internalized ^{125}I-(Tyr^2)-NDP were released from the cells into the medium during a 4-h incubation at 37°C (Fig. 4*A*). Greater than 75% of the internalized ^{125}I-(Tyr^2)-NDP activity was released from the cells within the first 2 h. However, no significant difference in cellular radioactive retention was found among these three radiolabeled analogues at 25°C incubation temperature (Fig. 4*B*). The radioactive moiety in the medium released from the cells was analyzed on a C-18 Sep-Pak column. Free $^{99m}TcO_4^-$ was rinsed off the column at 10% acetonitrile/H2O, whereas ^{125}I- and ^{99m}Tc-labeled peptides were eluted by 60% acetonitrile/H_2O. In media samples isolated from B16/F1 cells treated with ^{125}I-(Tyr^2)-NDP or ^{99m}Tc-labeled analogues, ~80% of the radioactivity was eluted with 10% acetonitrile/H_2O, suggesting that the majority of the radioactivity released from the cells into the media consisted of low molecular weight forms.

Bmax and Receptor Regulation. A Bmax of 4.562 and 5.812 fmol/0.5 million cells, representing about 5,500 and 7,000 receptors/per cell, was obtained for TXM-13 and B16/F1, respectively. α-MSH receptor regulation and turnover was examined in B16/F1 cells. B16/F1 cells were incubated for 24 h with NDP (20 or 50 nM) or with dialyzed FCS. The binding capacity of the treated cells for ^{125}I-(Tyr^2)-NDP *versus* incubation time at 25°C is shown in Fig. 5*A*. Compared with the control group, cell binding increased by ~20% for the cells cultured with media supplemented with 10% dialyzed FCS. The percentage of cell binding for the hormone-treated cells, both at 20 and 50 nM, was low at all time points over the 3-h incubation period. The binding capacity of the 50 nM NDP-treated cells for ^{125}I-(Tyr^2)-NDP did not completely recover until 96 h of incubation in normal media (Fig. 5*B*).

Murine Melanoma C57 Mouse Model. The *in vivo* biodistribution of the ^{99m}Tc- and ^{125}I-labeled α-MSH analogues were examined in healthy and tumor-bearing mouse models. Fig. 6 illustrates a comparison of the biodistribution properties among ^{99m}Tc-CCMSH, ^{99m}Tc-CGCG-NDP, and ^{125}I-(Tyr^2)-NDP in B16/F1 murine melanoma-bearing C57 mice at 4 h after injection. The tumor uptake for ^{99m}Tc-CCMSH was significantly higher than that of ^{99m}Tc-CGCG-NDP and ^{125}I-(Tyr^2)-NDP ($P < 0.001$ and $0.001 < P < 0.01$, respectively). The percentage of radioactivity in the blood of mice

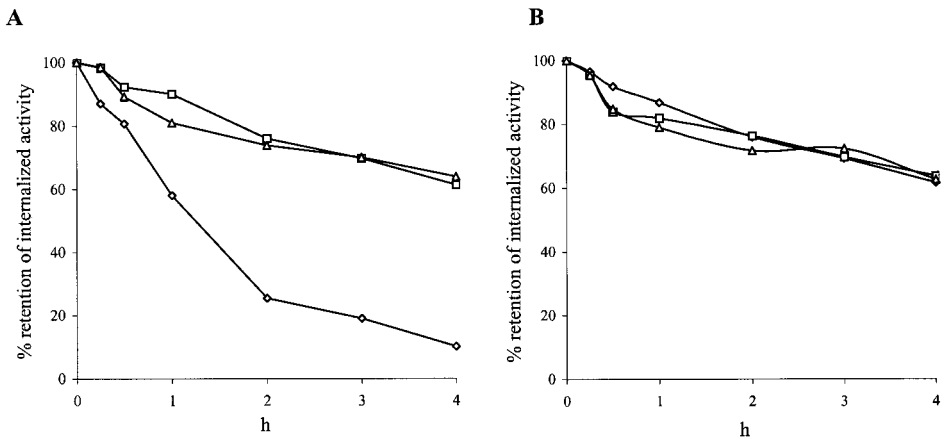

Fig. 4. The percentage of retention of internalized ^{99m}Tc-CCMSH (△), ^{99m}Tc-CGCG-NDP (□), and ^{125}I-(Tyr^2)-NDP (◇) radioactivity in B16/F1 cells over time at 37°C (*A*) or 25°C (*B*).

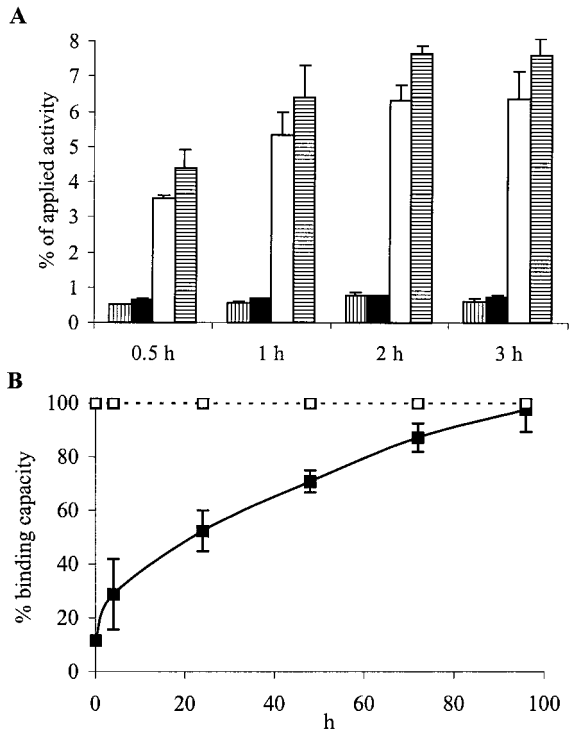

Fig. 5. Regulation of α-MSH receptor density by NDP. *A*, cell binding capacity of B16/F1 cells, cultured with 20 nM (▥) or 50 nM NDP (■) or with 10% dialyzed FCS (▤), for ^{125}I-(Tyr^2)-NDP. Bars, SD. *B*, recovery of ^{125}I-(Tyr^2)-NDP binding capacity in B16/F1 cells treated with 50 nM NDP (■). Control binding levels (□) of ^{125}I-(Tyr^2)-NDP were obtained with B16/F1 cells grown in media supplemented with 10% FCS. *Bars*, SD.

injected with ^{99m}Tc-CCMSH and ^{99m}Tc-CGCG-NDP was significantly lower than that of ^{125}I-(Tyr^2)-NDP ($P < 0.001$). The majority of the radioactivity for ^{99m}Tc-CCMSH and ^{125}I-(Tyr^2)-NDP was eliminated via the kidneys into the urine, whereas the radioactivity of ^{99m}Tc-CGCG-NDP was cleared from both urine and the GI tract. Because of the high tumor uptake and fast clearance, the tumor:blood uptake ratio for ^{99m}Tc-CCMSH was 6.3- and 21.5-fold higher than that of ^{99m}Tc-CGCG-NDP and ^{125}I-(Tyr^2)-NDP, respectively. However, the kidney uptake of ^{99m}Tc-CCMSH was 14.6 ± 1.9 (% ID/g), which was 5–12 times higher than that of ^{99m}Tc-CGCG-NDP and ^{125}I-(Tyr^2)-NDP.

Blockage of Nonspecific Kidney Uptake. Two strategies to decrease the high nonspecific renal radioactivity accumulation were investigated. One strategy was to reduce the amount of positive charge on CCMSH by substituting Lys with Nle or Gly. The IC_{50}s of Nle-CCMSH and Gly-CCMSH were determined by competitive binding assay with ^{125}I-(Tyr^2)-NDP in B16/F1 murine melanoma cells and compared with that of NDP (Table 2). The receptor binding affinity of the modified analogues was about 10 times lower than that of NDP, with IC_{50}s of 1.9, 3.8, and 0.21 nM for Nle^{11}-CCMSH, Gly^{11}-CCMSH, and NDP, respectively. However, the receptor binding affinity of the modified peptides did not change significantly compared with that of CCMSH (Table 2).

The results of biodistribution studies for the ^{99m}Tc-labeled modified peptides, ^{99m}Tc-Nle^{11}-CCMSH and ^{99m}Tc-Gly^{11}-CCMSH, compared with that of ^{99m}Tc-CCMSH in the murine melanoma C57 mouse model at 1 h after injection, are presented in Fig. 7. Although the kidney uptake of ^{99m}Tc-Nle-^{11}-CCMSH and ^{99m}Tc-Gly^{11}-CCMSH was dramatically decreased, their tumor uptake was also significantly lower than that of ^{99m}Tc-CCMSH ($P < 0.001$). There were also differences between these two modified peptides, with the tumor and kidney uptakes of ^{99m}Tc-Nle^{11}-CCMSH being significantly higher than those of ^{99m}Tc-Gly^{11}-CCMSH. In addition, the replacement of the Lys^{11} in CCMSH with Nle^{11} or Gly^{11} partially changed the path of the clearance from urine to GI. Greater than 50% ID of the radioactivity of ^{99m}Tc-Nle^{11}-CCMSH and ^{99m}Tc-Gly^{11}-CCMSH was cleared through the GI at 1 h after injection, whereas only about 20% ID was eliminated in urine (Fig. 7).

Another strategy to decrease the kidney uptake was lysine coinjection. Lysine coinjection has been shown to reduce nonspecific kidney retention associated with radiolabeled antibody fragments and peptides (34). Table 3 shows the results of the lysine coinjection for blocking the nonspecific kidney uptake of ^{99m}Tc-CCMSH in two different groups of healthy C57 mice at 30 min and 1 h after injection. Group 1 was first i.p. injected with 20 mg of lysine and then i.v. injected with a mixture of ^{99m}Tc-CCMSH and 25 mg of lysine, and group 2 was i.v. injected with a mixture of ^{99m}Tc-CCMSH and 25 mg of lysine only. There was no significant difference in the efficiency of reducing the kidney uptake between these two groups (Table 3). Hence, a single coinjection of ^{99m}Tc-CCMSH with 30 mg of lysine was performed in melanoma-bearing C57 mice to determine whether the lysine coinjection would interfere with the tumor uptake. Table 4 lists the biodistribution data of ^{99m}Tc-CCMSH with or without a 30-mg lysine coinjection in murine melanoma-bearing mice at 0.5, 1, 4, and 24 h after injection. Except for the kidney, the uptake values of ^{99m}Tc-CCMSH in both tumor and normal tissues of interest and the clearance kinetics were not significantly changed by the lysine coin-

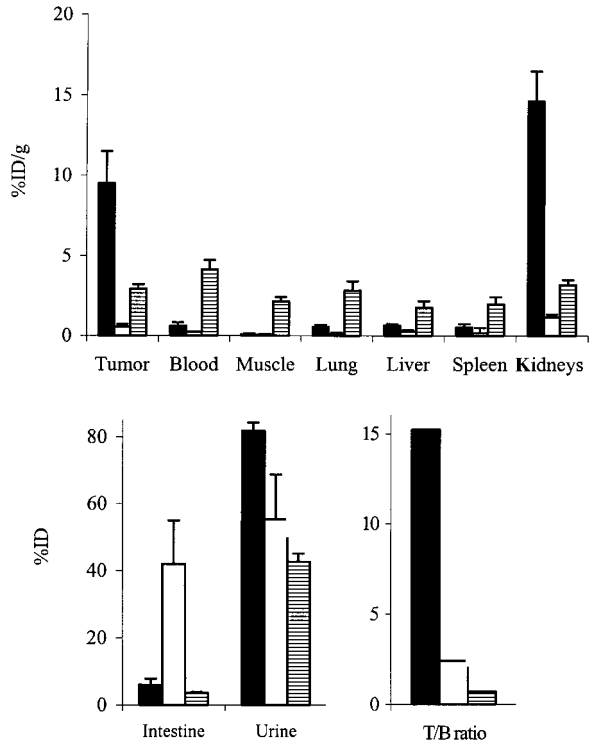

Fig. 6. Biodistribution comparison among ^{99m}Tc-CCMSH (■), ^{99m}Tc-CGCG-NDP (□), and ^{125}I-(Tyr^2)-NDP (▤) in B16/F1 murine melanoma bearing C57 mice at 4 h after injection ($n = 5$). The data are reported as % ID/g or % ID and tumor:blood uptake ratio (*T/B ratio*). *Bars*, SD.

Table 2 *The IC_{50} of α-MSH analogues*

Analogue	IC_{50} (M)
Gly^{11}-CCMSH	3.8×10^{-9}
Nle^{11}-CCMSH	1.9×10^{-9}
CCMSH	7.6×10^{-9}
ReCCMSH	2.9×10^{-9}
NDP	2.1×10^{-10}

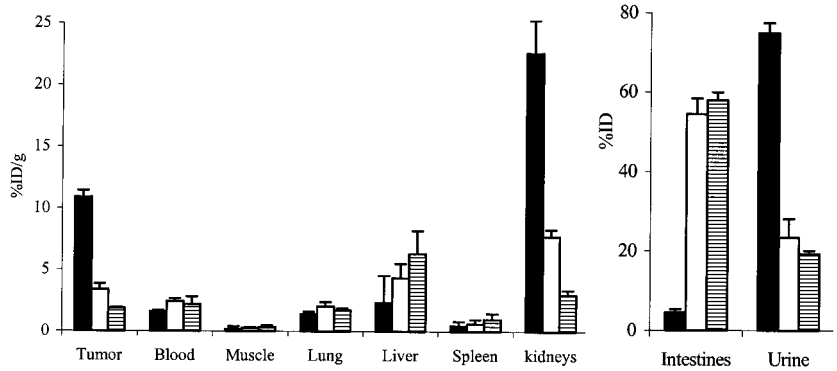

Fig. 7. Biodistribution and tumor targeting capacity of ^{99m}Tc-CCMSH (■), ^{99m}Tc-Nle^{11}-CCMSH (□), and ^{99m}Tc-Gly^{11}-CCMSH (▤) in B16/F1 murine melanoma-bearing C57 mice at 1 h after injection (n = 5; % ID/g or % ID). *Bars*, SD.

jection. Lysine coinjection was successful in reducing nonspecific kidney uptake by 48, 55, and 70% at 0.5, 1, and 4 h after injection, respectively (Table 4).

The *in vivo* specificity of ^{99m}Tc-CCMSH tumor uptake was investigated by coinjection of 2 μg of nonradiolabeled NDP with the radiolabeled peptide complex. Both groups of mice were also administered 30 mg of lysine to decrease the renal uptake. Coinjection of NDP specifically reduced the tumor uptake of ^{99m}Tc-CCMSH from 11.5 ± 1.3 to 1.8 ± 0.7 (% ID/g; $P < 0.001$) without changing the distribution of ^{99m}Tc-CCMSH in the normal tissues of interest (Fig. 8).

Tumor Imaging. A murine melanoma (B16/F1)-bearing C57 mouse was imaged at 1 and 8 h after the administration of ^{99m}Tc-CCMSH (Fig. 9). Although the radioactivity accumulation in the

Table 3 *Effect of lysine coinjection on the kidney uptake of ^{99m}Tc-CCMSH in C57 BL/6 mice at 30 min and 1 h after injection (n = 5; % ID/g or % ID)*

	30 min		1 h	
Tissues (% ID/g)	Group 1[a]	Group 2	Group 1	Group 2
Blood	2.11 ± 0.77	1.57 ± 0.59	1.18 ± 0.47	1.54 ± 0.53
Heart	1.06 ± 0.21	0.70 ± 0.33	0.62 ± 0.16	0.82 ± 0.34
Lungs	2.83 ± 0.68	2.14 ± 0.36	1.67 ± 0.76	2.07 ± 0.43
Spleen	0.87 ± 0.58	0.52 ± 0.25	0.58 ± 0.24	0.63 ± 0.44
Liver	1.67 ± 0.29	1.48 ± 0.34	1.47 ± 0.27	1.60 ± 0.49
Kidney	10.35 ± 0.43	10.84 ± 1.34	8.91 ± 1.72	11.01 ± 1.78
Pancreas	0.68 ± 0.12	0.36 ± 0.18	0.38 ± 0.11	0.52 ± 0.16
Muscle	0.74 ± 0.37	0.34 ± 0.17	0.46 ± 0.29	0.35 ± 0.07
% ID				
Blood	2.86 ± 0.85	1.88 ± 0.53	1.56 ± 0.46	1.96 ± 0.70
Stomach	0.25 ± 0.03	0.62 ± 0.86	0.32 ± 0.26	0.76 ± 0.81
Intestine	4.60 ± 0.53	4.78 ± 0.57	5.09 ± 1.12	4.47 ± 1.52
Kidney	3.21 ± 0.33	2.66 ± 0.36	2.49 ± 0.36	2.74 ± 0.40
Urine	65.14 ± 3.89	65.98 ± 13.6	75.12 ± 4.47	69.44 ± 12.89

[a] Group 1 received i.p. injections of 20 mg of lysine and after 5 min i.v. injections of a mixture of ^{99m}Tc-CCMSH and 25 mg of lysine. Group 2 received i.v. injections of a mixture of ^{99m}Tc-CCMSH and 25 mg of lysine only.

Table 4 *Biodistribution comparison of ^{99m}Tc-CCMSH with or without lysine coinjection in B16/F1 murine melanoma-bearing C57 BL/6 mice at various times after injection (% ID/g or % ID; n = 5)*

Tissues	30 min		1 h		4 h		24 h	
(% ID/g)	Lysine (−)	Lysine (+)	Lysine (−)	Lysine (+)	Lysine (−)	Lysine (+)	Lysine (−)	Lysine (+)
Tumor	12.97 ± 2.38	14.08 ± 1.22	11.64 ± 1.54	11.68 ± 1.55	9.51 ± 1.97	11.32 ± 3.25	1.38 ± 0.36	2.59 ± 0.83
Blood	3.28 ± 1.09	1.97 ± 0.27	1.26 ± 0.15	1.06 ± 0.49	0.62 ± 0.21	0.29 ± 0.27	0.06 ± 0.03	0.05 ± 0.03
Heart	1.55 ± 0.36	1.05 ± 0.37	0.49 ± 0.23	0.64 ± 0.57	0.25 ± 0.15	0.27 ± 0.17	0.13 ± 0.13	0.11 ± 0.06
Lungs	3.73 ± 0.86	3.19 ± 0.35	1.54 ± 0.25	1.54 ± 0.49	0.55 ± 0.12	0.32 ± 0.16	0.10 ± 0.06	0.16 ± 0.05
Spleen	0.92 ± 0.45	0.64 ± 0.23	0.54 ± 0.24	0.33 ± 0.26	0.54 ± 0.19	0.30 ± 0.25	0.18 ± 0.28	0.12 ± 0.12
Liver	2.36 ± 0.19	1.44 ± 0.29	1.79 ± 0.53	1.03 ± 0.37	0.65 ± 0.08	0.63 ± 0.16	0.06 ± 0.02	0.14 ± 0.05
Kidney	20.60 ± 2.42	10.74 ± 2.20[a]	19.71 ± 1.18	8.85 ± 2.25[b]	14.60 ± 1.88	4.45 ± 0.62[b]	1.22 ± 0.15	0.96 ± 0.27
Muscle	1.11 ± 0.47	0.69 ± 0.34	0.47 ± 0.52	0.15 ± 0.07	0.08 ± 0.06	0.16 ± 0.14	0.05 ± 0.05	0.03 ± 0.02
% ID								
Blood	3.07 ± 0.91	2.60 ± 0.43	1.20 ± 0.08	1.38 ± 0.64	0.65 ± 0.21	0.35 ± 0.32	0.07 ± 0.04	0.06 ± 0.04
Stomach	0.79 ± 0.24	0.53 ± 0.08	0.58 ± 0.15	0.52 ± 0.06	0.37 ± 0.20	0.28 ± 0.10	0.00 ± 0.00	0.06 ± 0.06
Intestine	3.16 ± 0.23	3.79 ± 0.27	4.53 ± 0.59	4.61 ± 0.71	6.03 ± 1.79	7.85 ± 1.74	0.15 ± 0.07	0.31 ± 0.22
Urine	57.48 ± 7.32	65.22 ± 3.36	67.18 ± 5.93	72.81 ± 7.75	81.83 ± 2.45[c]	81.84 ± 3.45[c]	98.36 ± 0.51[c]	97.12 ± 1.04[c]
Uptake ratio of tumor:normal tissue								
Tumor:blood	4.0	7.1	9.2	11.0	15.3	39.0	23.0	51.8
Tumor:muscle	11.7	20.4	24.8	77.8	118.8	70.7	27.6	86.0

[a] $0.05 > P > 0.01$.
[b] $P < 0.01$.
[c] Urine + feces.

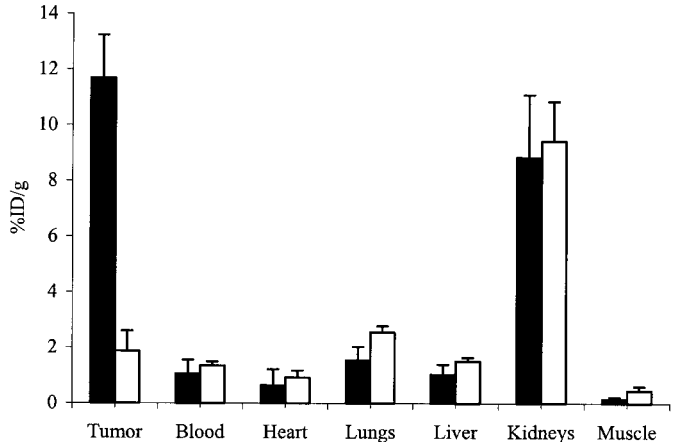

Fig. 8. *In vivo* tumor targeting specificity of ^{99m}Tc-CCMSH. Two to 4 μCi of ^{99m}Tc-CCMSH + 30 mg lysine were injected with 2 μg of NDP (□) or without NDP (■) in B16/F1 melanoma-bearing C57 mice at 1 h after injection (n = 5). *Bars*, SD.

bladder is very high, the tumor spot is identifiable 1 h after injection image (Fig. 9, *left*). After the mouse voids its bladder contents, the extremely high tumor uptake and low background in the normal tissues are observed as illustrated in the image obtained 8 h after injection of radioactivity (Fig. 9, *right*).

Human Melanoma Scid Mouse Model. The tumor uptake property of ^{99m}Tc-CCMSH was further examined in the amelanonic TXM-13 and melanonic TXM-13JQ human melanoma-bearing Scid mouse models. Table 5 shows the biodistribution, tumor uptake, and tumor:tissue uptake ratios of ^{99m}Tc-CCMSH in TXM-13 human melanoma bearing Scid mice at 30 min, 1, 4, and 24 h after injection with or without lysine coinjection. The biodistribution of the ^{99m}Tc-CCMSH in normal tissues of interest was comparable between the two mouse models (*e.g.*, TXM-13 human melanoma-bearing Scid mice and B16/F1 murine melanoma-bearing C57 mice; Tables 4 and 5). Compared with murine melanoma, the tumor uptake of ^{99m}Tc-CCMSH in human melanoma was lower, which may be attributable to its lower receptor density and differences in *in vivo* behavior. However, a tumor uptake of 2.39 ± 0.42% ID/g was obtained at 4 h after injection in TXM-13 melanoma-bearing Scid mice, resulting in an uptake ratio of tumor:normal tissue of 11.5 and 50.9 for the blood and the muscle, respectively (Table 5). Biodistribution results of ^{99m}Tc-CCMSH in Scid mice bearing the melanonic TXM-13JQ human melanoma at 30 min and 4 h after injection are illustrated in Fig. 10. The tumor uptake at both 30 min and 4 h after injection was (7.64 ± 2.12 and 6.55 ± 1.31, respectively), significantly higher than that in Scid mice bearing the amelanonic solid TXM-13 human melanoma ($0.001 < P < 0.01$ and $P < 0.001$, respectively).

Tumor Tissue Histopathological Studies. Histopathological examinations were performed on tumors induced by s.c. injection of B16/F1 murine melanoma cells and TXM-13 and TXM-13JQ human melanoma tumor cells. Tumor sections from the histopathological studies are shown Fig. 11. All of the three pictures show unencapsulated masses composed of round cells with distinct borders, moderate basophilic cytoplasm, often containing brown to black intracytoplasmic pigment granules. The cells are also marked by anisokaryosis of the round nucleoli, which are consistent with malignant melanoma. Morphologically, the B16/F1- and TXM-13JQ-induced tumors formed melanonic gelatinous masses, whereas TXM-13 induced an amelanonic solid mass tumor. Moreover, severe necrosis was observed in the amelanonic solid TXM-13 human melanoma tumor (Fig. 11*C*), whereas necrosis was much less prevalent in the TXM-13JQ tumor tissue and rarely seen in the B16 tumor (Fig. 11, *A* and *B*).

DISCUSSION

Cellular internalization of a bioactive complex, such as antibody or peptide, is often subject to extensive metabolization in the lysosome (35). Redistribution of the radioactive catabolites of the radiocomplex, having been degraded in target cells, will dramatically influence the tumor radioactivity uptake and retention (36). It has been demonstrated that some radioactive catabolites, such as free iodine and iodobenzoic acid, are rapidly washed out from targeted cells. For example, the tumor radioactivity retention time for a radioiodinated internalizing antibody is significantly shorter than the same molecule labeled with a radiometal chelate, such as ^{111}In (37).

In this investigation, the data illustrated that ~70% of the membrane-bound radiolabeled α-MSH analogues were internalized in both B16/F1 murine (Fig. 3) and TXM-13 human melanoma cell lines (data not shown). Although there was no difference in cellular retention between these three radiolabeled analogues at 25°C, the cellular retention of the ^{99m}Tc-labeled analogues was 2.5-fold higher than that of the radioiodinated analogue at 37°C (Fig. 4). C-18 Sep-Pak column

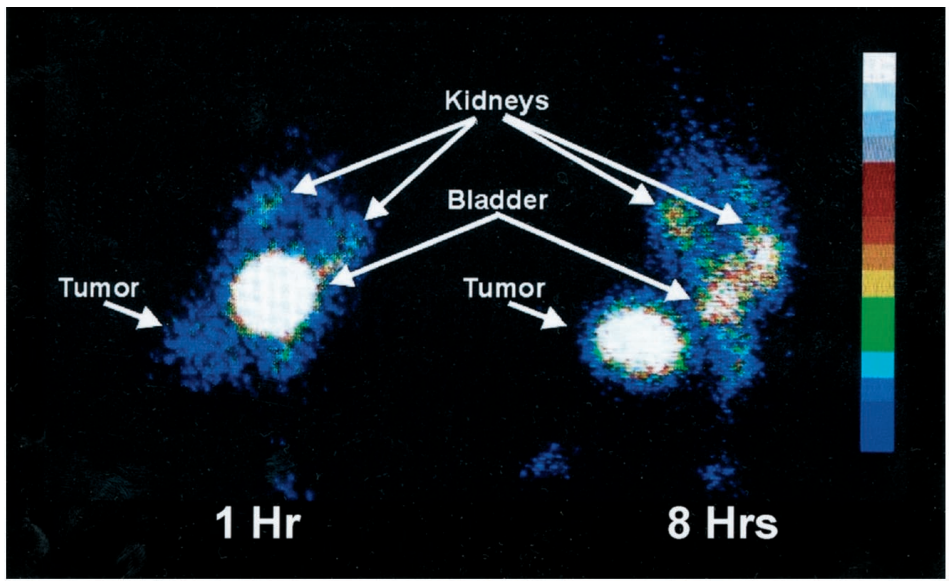

Fig. 9. Imaging of B16/F1 murine melanoma-bearing C57 mouse after 1 h (*left*) and 8 h (*right*) administration of 100 μCi of ^{99m}Tc-CCMSH.

Table 5 *Biodistribution comparison of ^{99m}Tc-CCMSH with or without lysine coinjection in TXM-13 human melanoma-bearing Scid mice at various times after injection (% ID/g or % ID; n = 5)*

Tissues	30 min		1 h		4 h		24 h	
(% ID/g)	Lysine (−)	Lysine (+)	Lysine (−)	Lysine (+)	Lysine (−)	Lysine (+)	Lysine (−)	Lysine (+)
Tumor	3.08 ± 0.58	4.63 ± 1.02	3.26 ± 0.77	4.05 ± 0.19	2.22 ± 0.25	2.39 ± 0.42	0.48 ± 0.12	0.59 ± 0.11
Blood	2.67 ± 0.33	3.28 ± 0.97	1.41 ± 0.37	1.01 ± 0.18	0.38 ± 0.05	0.22 ± 0.04	0.15 ± 0.04	0.13 ± 0.01
Heart	0.93 ± 0.11	1.29 ± 0.35	0.62 ± 0.24	0.34 ± 0.16	0.16 ± 0.12	0.12 ± 0.16	0.00 ± 0.00	0.10 ± 0.03
Lungs	2.89 ± 0.47	4.44 ± 1.33	1.85 ± 0.44	1.40 ± 0.25	0.38 ± 0.05	0.22 ± 0.06	0.06 ± 0.05	0.14 ± 0.03
Spleen	0.68 ± 0.30	1.21 ± 0.51	0.39 ± 0.28	0.25 ± 0.23	0.27 ± 0.07	0.24 ± 0.14	0.13 ± 0.12	0.19 ± 0.15
Liver	2.02 ± 0.52	2.86 ± 0.77	1.54 ± 0.39	1.82 ± 0.35	1.11 ± 0.39	0.27 ± 0.05	0.19 ± 0.02	0.18 ± 0.02
Kidney	18.10 ± 2.19	13.58 ± 2.67[a]	23.72 ± 3.04	10.50 ± 0.82[b]	10.49 ± 2.27	6.74 ± 0.60[a]	1.47 ± 0.12	0.93 ± 0.12[a]
Muscle	0.40 ± 0.09	0.76 ± 0.18	0.29 ± 0.07	0.14 ± 0.11	0.04 ± 0.02	0.07 ± 0.05	0.02 ± 0.00	0.03 ± 0.02
% ID								
Blood	4.36 ± 0.67	5.29 ± 1.24	2.44 ± 0.53	1.60 ± 0.32	0.63 ± 0.07	0.34 ± 0.07	0.21 ± 0.04	0.22 ± 0.02
Stomach	0.96 ± 0.88	0.63 ± 0.11	1.68 ± 0.40	0.65 ± 0.26	0.38 ± 0.08	0.24 ± 0.26	0.11 ± 0.06	0.15 ± 0.09
Intestine	8.08 ± 0.79	8.90 ± 2.43	7.25 ± 0.75	12.78 ± 3.24	11.68 ± 0.70	13.05 ± 4.26	1.02 ± 0.88	0.38 ± 0.12
Urine	58.78 ± 5.70	45.32 ± 11.37	61.48 ± 6.55	61.01 ± 4.96	78.68 ± 1.33[c]	76.66 ± 8.85[c]	97.00 ± 0.94[c]	97.73 ± 0.31[c]
Uptake ratio of tumor:normal tissue								
Tumor:blood	1.15	1.44	2.03	4.11	5.82	11.52	3.31	4.56
Tumor:muscle	7.89	6.17	11.55	19.14	38.71	50.90	27.50	37.14

[a] $0.05 > P > 0.01$.
[b] $P < 0.01$.
[c] Urine + feces.

analysis of the radioactive moiety in the medium showed that the majority of the radioactivity released from the cells into the media had been metabolized into low molecular weight forms. No differences in the cellular retention of ^{99m}Tc-CCMSH and ^{99m}Tc-CGCG-NDP were found *in vitro*, contradicting the results observed *in vivo* (Fig. 6), which might be attributable to differences in metabolism of the radiolabeled complexes *in vitro* and *in vivo*.

The results of NDP-induced down-regulation of α-MSH receptors on B16/F1 cells (Fig. 5) were consistent with previous reports (38, 39), which suggested that α-MSH peptides are internalized together with their receptors upon binding. The use of dialyzed FCS eliminated trace levels of α-MSH hormone in the FCS supplemented media, resulting in a slight increase in B16/F1 cell receptor binding of ^{125}I-(Tyr^2)-NDP. However, the treatment of the B16/F1 cells with NDP at a concentration of as low as 20 nM blocked α-MSH receptor-mediated binding of the iodinated NDP analogue, illustrating sensitivity of the receptor for its cognate ligand. Receptor internalization and slow recovery highlight the importance of developing a α-MSH receptor targeting agent that not only possess high affinity but also an equally high degree of cellular retention.

In this study, a cell binding value of 4−8% was obtained for all three radiolabeled analogues, which is significantly lower than the percentage of cell binding values reported for radiolabeled antibodies (40). The difference in percentage of cell binding values between ^{99m}Tc-CCMSH and radiolabeled antibodies is primarily attributable to the concentration of receptor or antigen. To illustrate the effect of receptor concentration on the binding capacity, the binding fraction (1/*r*) of ^{125}I-(Tyr^2)-NDP to B16/F1 cells was tested by an immunoreactivity assay, commonly used to determine the bioactivity of a radiolabeled antibody (33). A binding fraction (1/*r*) of 0.37 was obtained for the radioiodinated NDP (2,000 Ci/mmol) to B16/F1 cells. Because the receptor density on B16/F1 cells was 7,000/cell, a cell concentration of 32 million cells/ml represented a receptor concentration of 0.37 nM, which was approximately the *Ki* of NDP. Hence, the low percentage of cell binding for ^{125}I-(Tyr^2)-NDP observed in this investigation (Fig. 3) was attributable to the low receptor concentration on the cells (*e.g.*, 0.2 million cells/0.5 ml only represented a receptor concentration of 4.6 pM, which is ~45 times lower than the *Ki* of NDP). This result demonstrates that the immunoreactivity assay is difficult to apply when receptor concentration is low.

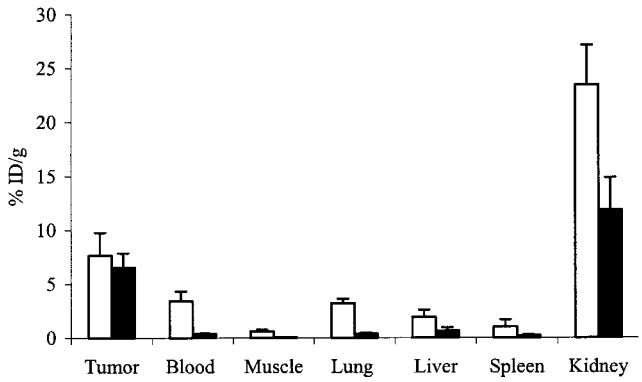

Fig. 10. Biodistribution and tumor uptake of ^{99m}Tc-CCMSH in TXM-13JQ human melanoma-bearing Scid mice at 30 min (□) and 4 h (■) after injection ($n = 5$; % ID/g). *Bars*, SD.

The *in vivo* results showed that the tumor uptake of ^{99m}Tc-CCMSH was significantly higher than that of ^{99m}Tc-labeled and radioiodinated linear NDP analogues in the murine melanoma mouse model. The tumor:blood uptake ratio of ^{99m}Tc-CCMSH at 4 h after the injection time point was 6.3- and 21.5-fold higher than that of ^{99m}Tc-CGCG-NDP and ^{125}I-(Tyr^2)-NDP, respectively (Fig. 6). This result was consistent with our previous report that the radiolabeled linear α-MSH analogues were rapidly washed out of the tumor tissue (31). In comparison with the linear analogues, ^{99m}Tc-CCMSH is cyclized via the site-specific metal coordination by three Cys^{3,4,10} sulfhydryls and a Cys^4 amide nitrogen (23, 32). The cyclized and compacted structure of ^{99m}Tc-CCMSH appears to enhance the resistance of the molecule to proteolysis and contributes significantly to the high *in vivo* tumor uptake and retention. The high tumor uptake of ^{99m}Tc-CCMSH was shown to be specific, because 84% of the tumor uptake was identically blocked by coinjection of 2 μg of nonradiolabeled NDP (Fig. 8). The extremely high tumor uptake and retention of ^{99m}Tc-CCMSH is also identified in the 8-h postinjection imaging (Fig. 9).

The nonspecific radioactivity accumulation in the kidneys is often associated with the *in vivo* application of radiolabeled peptides and antibody fragments (23, 28, 34). It was hypothesized that the positive charge of the lysine residue in the ^{99m}Tc-CCMSH sequence contributed significantly to the nonspecific radioactivity kidney retention.

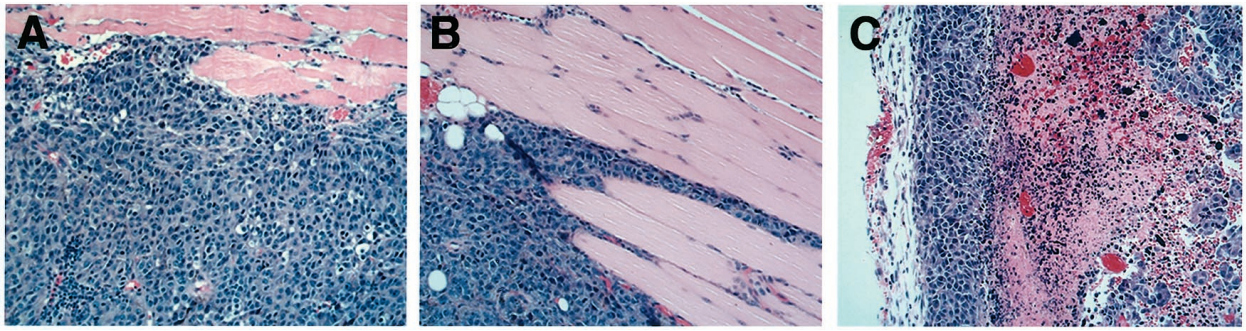

Fig. 11. Histopathological studies of melanonic gelatinous B16/F1 murine melanoma tissue (*A*), melanonic gelatinous TXM-13JQ (*B*), and amelanonic solid TXM-13 (*C*) human melanoma tissues.

Substitution of Lys^{11} with Nle^{11} or Gly^{11} in the ^{99m}Tc-CCMSH sequence yielded analogues with reduced kidney uptake (Fig. 7), but the tumor uptake of the two analogues was also significantly lower compared with that of ^{99m}Tc-CCMSH. Although the Nle^{11}-CCMSH and Gly^{11}-CCMSH analogues showed similar receptor binding affinities to CCMSH *in vitro* (Table 2), the loss of the lysine residue at position 11 adversely affected tumor uptake *in vivo* (Fig. 7). These results demonstrate that the lysine residue in ^{99m}Tc-CCMSH is critical for effective melanoma targeting *in vivo*. Moreover, the Lys^{11} replacement in ^{99m}Tc-CCMSH altered the pathway of clearance from urine to the GI tract, which slowed the clearance kinetics of the ^{99m}Tc-labeled analogues from the whole body. However, nonspecific kidney retention of ^{99m}Tc-CCMSH was effectively reduced by lysine coinjection. A single injection of 30 mg of lysine together with the ^{99m}Tc-CCMSH decreased the kidney uptake by 48, 55, and 70% at 30 min and 1 and 4 h after injection without altering tumor uptake. Lysine coinjection showed more efficient blocking at 4 h after injection, suggesting that part of the radioactivity in the kidney at earlier time points was attributable to radioactivity clearance from the kidney into the urine. Kidney uptake with the lysine coinjection was lower, but without statistical difference ($P > 0.05$), than that of the control group at 24 h after radiocomplex administration (Table 4).

Substantial tumor uptake of ^{99m}Tc-CCMSH was also demonstrated in the TXM-13 and TXM-13JQ human melanoma-bearing Scid mice models (Table 5; Fig. 10). The biodistribution of ^{99m}Tc-CCMSH in normal tissue in TXM-13 human melanoma-bearing Scid mice was similar to that in B16/F1 murine melanoma-bearing C57 mice (Tables 4 and 5). It appeared that the lower α-MSH receptor density and tumor morphology contributed to the reduced tumor uptake of ^{99m}Tc-CCMSH in the TXM-13 human melanoma xenografts compared with that in the B16/F1 murine melanoma in the C57 mouse model. There was a significant difference in uptake of ^{99m}Tc-CCMSH between TXM-13- and TXM-13JQ-induced human melanoma tumors. Tumor uptake of ^{99m}Tc-CCMSH at 4 h after injection increased from 2.39 ± 0.41 (% ID/g) in TXM-13 to 6.55 ± 1.31 (% ID/g) in TXM-13JQ. The TXM-13JQ cell line was derived from the original TXM-13 cell line by successive passaging *in vitro*. *In vivo* TXM-13JQ formed uniform melanonic gelatinous tumors with limited necrotic centers in contrast to TXM-13, which formed amelanonic solid tumors with extensive necrotic centers (Fig. 11). Clearly, the extent of necrosis within the TXM-13 human melanoma affects the tumor uptake. However, even in the solid TXM-13 human melanoma Scid mouse model, the uptake ratio of tumor:blood or tumor:muscle of 11.5 or 50.9, respectively, was obtained for ^{99m}Tc-CCMSH at 4 h after injection because of the high tumor uptake and low background in the normal tissues (Table 5).

In conclusion, the cyclic α-MSH analogue ^{99m}Tc-CCMSH showed superior tumor uptake and retention and fast whole body clearance in both murine and human melanoma mouse models, compared with any other radiolabeled α-MSH analogue (14, 25–31). The compacted cyclic structure of ^{99m}Tc-CCMSH (23, 32) exhibits resistance to degradation and enhanced intracellular retention, resulting in the high *in vivo* tumor-targeting properties of the molecule. Lysine coinjection rather than peptide modification of the Lys^{11} residue in ^{99m}Tc-CCMSH was shown to significantly decrease the nonspecific radioactivity accumulation in the kidneys without significantly interfering with the high melanoma-targeting properties of ^{99m}Tc- CCMSH. The metal-cyclized CCMSH molecule displays high potential for the development of melanoma-specific diagnostic and therapeutic agents.

ACKNOWLEDGMENTS

We express our gratitude to Dr. Wynn Volkert and Dr. Susan Deutscher for helpful discussions; Dr. Nellie K. Owen, Dr. Vladislav V. Glinskii, Chys Higginbothan, Julia Robinson, and Donna Whitener for assistance; and Dr. Isaiah J. Fidler for kindly supplying the TXM-13 human melanoma cell line.

REFERENCES

1. Marghood, A. A., Slade, J., Salopek, T. G., Kopf, A. W., Bart, R. S., and Rigel, D. S. Basal cell and squamous cell carcinomas are important risk factors for cutaneous malignant melanoma. Cancer (Phila.), *75:* 707–714, 1995.
2. Anderson, C. M., and Buzaid, A. C. Systemic treatments for advanced cutaneous melanoma. Oncology, *9:* 1149–1158, 1995.
3. Larson, S. M., Brown, J. P., Wright, P. W., Carrasquillo, J. A., Hellstrom, I., and Hellstrom, K. E. Imaging of melanoma with I-131-labeled monoclonal antibodies. J. Nucl. Med., *24:* 123–129, 1983.
4. Wahl, R. L., Swanson, N. A., Johnson, J. W., Natale, R., Petry, N. A., Mallette, S., Kasina, S., Reno, J., Sullivan, K., and Abrams, P. Clinical experience with Tc-99m labeled (N_2S_2) anti-melanoma antibody fragments and single photon emission computed tomography. Am. J. Physiol. Imaging, *7:* 48–58, 1992.
5. Loeffler, K. U., Brautigam, P., Simon, J. C., Althauser, S. R., Wuttig, C., and Witschel, H. Immunoscintigraphy for ocular melanoma: a reliable diagnostic technique? Graefe's Arch. Clin. Exp. Ophthalmol., *234:* 100–104, 1996.
6. Cornelius, E. A., Neumann, R. D., and Zoghbi, S. S. Intrapatient and interpatient comparison of tumor size and monoclonal antibody uptake in melanoma. Clin. Nucl. Med., *13:* 243–249, 1988.
7. Serafini, A. N., Kotler, J., Feun, L., Dewanjee, M., Robinson, D., Salk, D., Sfakianakis, G., Abrams, P., Savaraj, N., and Goodwin, D. Technetium-99m labeled monoclonal antibodies in the detection of metastatic melanoma. Clin. Nucl. Med., *14:* 580–587, 1989.
8. Halpern, S. E., and Bartholomew, R. Pharmacokinetics of an indium-111-labeled IgG monoclonal antibody over a prolonged period. Eur. J. Nucl. Med., *22:* 1323–1325, 1995.
9. Carrasquillo, J. A., Abrams, P. G., Schroff, R. W., Reynolds, J. C., Woodhouse, C. S., Morgan, A. C., Keenan, A. M., Foon, K. A., Perentesis, P., and Marshall, S. Effect of antibody dose on the imaging and biodistribution of In-111 9.2.27 anti-melanoma monoclonal antibody. J. Nucl. Med., *29:* 39–47, 1988.
10. Kwok, C. S., Cole, S. E., and Liao, S. K. Uptake kinetics of monoclonal antibodies by human melanoma multicell spheroids. Cancer Res., *48:* 1856–1863, 1988.
11. Ong, G. L., and Mattes, M. J. Penetration and binding of antibodies in experimental human solid tumors grown in mice. Cancer Res., *49:* 4264–4273, 1989.
12. Frontiera, M., Murray, J. L., Lamki, L., Thomas, J., Satterlee, W., Schmelter, R., Rosenblum, M. G., Khazaeli, M. B., Unger, M. W., and Robinson, W. A. Sequential use of indium-111 labeled monoclonal antibodies 96.5 and ZME-018 does not increase detection sensitivity of metastatic melanoma. Clin. Nucl. Med., *14:* 357–366, 1989.

13. Bakker, W. H., Krenning, E. P., Reubi, J. C., Breeman, W. A. P., Setyono-Han, B., de Jong, M., Kooij, P. P. M., Bruns, C., van Hagen, P. M., Marbach, P., Visser, T. J., Pless, J., and Lamberts, S. W. J. *In vivo* application of (^{111}In-DTPA-D-Phe)-octreotide for detection of somatostatin receptor-positive tumors in rat. Life Sci., *49:* 1593–1601, 1991.
14. Bard, D. P., Knight, C. G., and Page-Thomas, D. P. A chelating derivative of α-melanocyte stimulating hormone as a potential imaging agent for malignant melanoma. Br. J. Cancer, *62:* 919–922, 1990.
15. Tatro, J. B., and Reichlin, S. Specific receptors for α-melanoma stimulating hormone are widely distributed in tissues of rodents. Endocrinology, *121:* 1900–1907, 1987.
16. Siegrist, W., Solca, F., Stutz, S., Giuffre, L., Carrel, S., Girard, J., and Eberle, A. N. Characterization of receptors for α-melanocyte stimulating hormone on human melanoma cells. Cancer Res., *49:* 6352–6358, 1989.
17. Tatro, J. B., Atkins, M., Mier, J. W., Hardarson, S., Wolfe, H., Smith, T., Entwistle, M. L., and Reichlin, S. Melanotropin receptors demonstrated *in situ* in human melanoma. J. Clin. Investig., *85:* 1825–1832, 1990.
18. Cone, R. D., Mountjoy, K. G., Robbins, L. S., Nadeau, J. H., Johnson, K. R., Roselli-Rehfuss, L., and Mortrud, M. T. Cloning and functional characterization of a family of receptors for the melanotropin peptides. Ann. NY Acad. Sci., *680:* 342–363, 1993.
19. Saywer, T. K., Sanfilippo, P. J., Hruby, V. J., Engel, M. H., Heward, C. B., Burnett, J. B., and Hadley, M. E. 4-Norleucine, 7-D-phenylalanine-α-melanocyte-stimulating hormone: a highly potent α-melanotropin with ultralong biological activity. Proc. Natl. Acad. Sci. USA, *77:* 5754–5758, 1980.
20. Cody, W. L., Mahoney, M., Knittle, J. J., Hruby, V. J., Castrucci, A. M., and Hadley, M. E. Cyclic melanotropin 7-D-phenylalanine analogs of active-site sequence. J. Med. Chem., *28:* 583–588, 1985.
21. Al-Obeidi, F., Castrucci, A. M. L., Hadley, M. E., and Hruby, V. J. Potent and prolonged acting cyclic lactam analogs of α-melanotropin: design based on molecular dynamics. J. Med. Chem., *32:* 2555–2561, 1989.
22. Hruby, V. J., Lu, D., Sharma, S. D., Castrucci, A. L., Kesterson, R. A., Al-Obeidi, F. A., Hadley, M. E., and Cone, R. D. Cyclic lactam α-melanotropin analogues of Ac-Nle^4-Cyclo[Asp^5, D-Phe^7, Lys^{10}]α-melanocyte-stimulating hormone-(4–10)-NH_2 with bulky aromatic amino acids at position 7 show high antagonist potency and selectivity at specific melanocortin receptors. J. Med. Chem., *38:* 3454–3461, 1995.
23. Giblin, M. F., Wang, N., Hoffman, T. J., Jurisson, S. S., and Quinn, T. P. Design and characterization of α-melanotropin peptide analogs cyclized though rhenium and technetium metal coordination. Proc. Natl. Acad. Sci. USA, *95:* 12814–12818, 1998.
24. Morandini, R., Vargha, H. S., Libert, A., Loir, B., Botyanszki, J., Medzihradszky, K., and Ghanem, G. Receptor-mediated cytotoxicity of α-MSH fragments containing melphalan in a human melanoma cell line. Int. J. Cancer, *56:* 129–133, 1994.
25. Siegrist, W., Oestreicher, M., Stutz, S., Girard, J., and Eberle, A. E. Radio-receptor assay for α-MSH using mouse B16 melanoma cells. J. Recept. Res., *8:* 323–343, 1988.
26. Garg, P. K., Alston, K. L., Welsh, P. C., and Zalutsky, M. R. Enhanced binding and inertness to dehalogenation of α-melanotropin peptides labeled using *N*-succinimidyl 3-iodobenzoate. Bioconjugate Chem., *7:* 233–239, 1996.
27. Vaidyanathan, G., and Zalutsky, M. R. Fluorine-18-labeled [Nle^4, D-Phe^7]-α-MSH, an α-melanocyte stimulating hormone analog. Nucl. Med. Biol., *24:* 171–178, 1997.
28. Wraight, E. P., Bard, D. R., Maughan, C. G., Knight, C. G., and Page-Thomas, D. P. The use of a chelating derivative of α-melanocyte stimulating hormone for the clinical imaging of malignant melanoma. Br. J. Radiol., *65:* 112–128, 1992.
29. Bagutti, C., Stolz, B., Albert, R., Bruns, C., Pless, J., and Eberle, A. N. ^{111}In-DPTA-labeled analogs of α-melanocyte-stimulating hormone for melanoma targeting: receptor binding *in vitro* and *in vivo*. Int. J. Cancer, *58:* 749–755, 1994.
30. Giblin, M. F., Jurisson, S. S., and Quinn, T. P. Synthesis and characterization of rhenium-complexed-melanotropin analogs. Bioconjugate Chem., *8:* 347–353, 1997.
31. Chen, J. Q., Giblin, M. F., Wang, N., Jurisson, S. S., and Quinn, T. P. *In vivo* evaluation of ^{99m}Tc/^{188}Re-labeled α melanocyte stimulating hormone analogs for specific melanoma targeting. Nucl. Med. Biol., *26:* 687–693, 1999.
32. Chen, J. Q., Wang, N., Jurisson, S. S., and Quinn, T. P. Biodistribution properties of linear and cyclic ^{99m}Tc-labeled α-melanotropin peptides. *In:* M. Nicolini and U. Mazzi (eds.), Technetium, Rhenium and Other Metals in Chemistry and Nuclear Medicine, pp. 457–463. Padova, Italy: SG Editoriali, 1998.
33. Lindmo, T., Boven, E., Cuttitta, F., Fedorko, J., and Bunn, P. A., Jr. Determination of the immunoreactive fraction of radiolabeled monoclonal antibodies by linear extrapolation to binding at infinite antigen excess. J. Immunol. Methods, *72:* 77–89, 1984.
34. Lang, L., Jagoda, E., Wu, C. H., Brechbiel, M. W., Gansow, O. A., Pastan, I., Park, C. H., Carrasquillo, J. A., and Eckelman, W. C. Factors influencing the *in vivo* pharmacokinetics of peptides and antibody fragments: the pharmacokinetics of two PET-labeled low molecular weight proteins. Q. J. Nucl. Med., *41:* 53–61, 1997.
35. Mattes, M. J., Griffiths, G. L., Diril, H., Goldenberg, D. M., Ong, G. L., and Shih, L. B. Processing of antibody-radioisotope conjugates after binding to the surface of tumor cells. Cancer (Phila.), *69:* 502–507, 1994.
36. Fritzberg, A. R., and Beaumier, P. L. Targeted proteins for diagnostic imaging: does chemistry make a difference? J. Nucl. Med., *33:* 394–396, 1992.
37. Chen, J. Q. Radiolabeling and biotinylation of internalizing monoclonal antibody chimeric BR96: potential use for extracorporeal immunoadsorption with enhanced tumor radioactivity retention of iodine, indium and rhenium (Doctoral Dissertation). Bloms I Lund (Sweden), 30–43, 1996.
38. Wong, W., and Minchin, R. F. Binding and internalization of melanocyte stimulating hormone receptor ligand [Nle^4,D-Phe^7]α-MSH in B16 melanoma cells. Int. J. Biochem. Cell Biol., *28:* 1223–1232, 1996.
39. Siegrist, W., Stutz, S., and Eberle, A. N. Homologous and heterologous regulation of α-melanocyte-stimulating hormone receptor in human and mouse melanoma cell lines. Cancer Res., *54:* 2604–2610, 1994.
40. Hellstrom, I., Garrigues, H. J., Garrigues, U., and Hellstrom, K. E. Highly tumor-reactive, internalization, mouse monoclonal antibodies to Ley-related cell surface antigens. Cancer Res., *50:* 2183–2190, 1990.

Melanoma-targeting Properties of ^{99m}Technetium-labeled Cyclic α-Melanocyte-stimulating Hormone Peptide Analogues

JianQing Chen, Zhen Cheng, Timothy J. Hoffman, et al.

Cancer Res 2000;60:5649-5658.